JOC The Journal of Organic Chemistry

ARTICLE

pubs.acs.org/joc

Palmarumycins BG1−BG7 and Preussomerin BG1: Establishment of Their Absolute Configurations Using Theoretical Calculations of Electronic Circular Dichroism Spectra

You-Sheng Cai,[†] Tibor Kurtán,[‡,*] Ze-Hong, Miao,[†] Attila Mándi,[§] István Komáromi,[∥] Hai-Li Liu,[†] Jian Ding,[†] and Yue-Wei Guo*[,†]

[†]State Key Laboratory of Drug Research Institute of Materia Medica Chinese Academy of Sciences, Zu Chong Zhi Road 555 Zhangjiang Hi-Tech Park, Shanghai 201203, P. R. China

[‡]Department of Organic Chemistry, University of Debrecen, POB 20, 4010 Debrecen, Hungary

[§]Research Group for Carbohydrates Hungarian Academy of Sciences University of Debrecen, POB 94, 4010 Debrecen, Hungary

[∥]Thrombosis, Hemostasis and Vascular Biology Research Group, Hungarian Academy of Sciences, University of Debrecen, Nagyerdei krt. 98, 4032 Debrecen, Hungary

Supporting Information

ABSTRACT: Palmarumycins BG1−BG7 (**1**−**7**), seven new compounds related to palmarumycins, were isolated from the aerial parts of *Bruguiera gymnorrhiza* as well as a new preussomerin derivative BG1 (**8**). The structures of these compounds were determined mainly by the analysis of their NMR and MS data, and their relative configurations were assigned on the basis of their $^{3}J_{H,H}$ coupling constants. Compounds **4** and **7** have a sulfate group that is unprecedented among members of spirodioxynaphthalene-type natural products. The absolute configurations of **1**−**8** were determined by TDDFT CD calculations of the solution conformers. Compound **5** displayed inhibitory activity against HL 60 and MCF-7 cell lines.

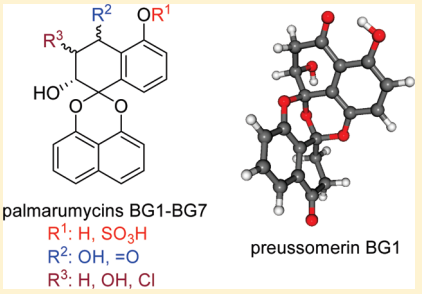

INTRODUCTION

Preussomerins and palmarumycins belong to a structurally remarkable class of natural products mainly isolated from various fungal cultures. Because of its interesting structural patterns and important biological properties, a large number of investigations on this family have been carried out in the last 20 years.[1] Preussomerins structurally consist of two unsaturated decalin units connected via three oxygen bridges through two spiroketal carbons, one located at the upper decalin unit and the other at the lower decalin unit. Palmarumycins lack one of the bridged oxygens and have a 1,8-dioxynaphthalene ring instead of the tetralone moiety. These metabolites display a wide range of biological activities, including antibacterial,[3,4,7,8] antifungal,[2,4,7,9] algicidal,[5] nematicidal,[10] and antileishmanial effects,[11] phospholipase D inhibitory,[12] FPTase inhibitory,[6] and antitumor activity.[13]

As a part of our ongoing research toward the discovery of biologically active metabolites from Chinese marine organisms, we continued the investigation of *Bruguiera gymnorrhiza*. Prior investigations of *B. gymnorrhiza* in our group have afforded a variety of novel bioactive metabolites.[14−18] In the course of the present work, we obtained seven new spirodioxynaphthalene compounds, which were named palmarumycins BG1−BG7 (**1**−**7**), along with one new preussomerin derivative BG1 (**8**).[6] In this paper, we describe the isolation, structure elucidation, and biological activity of metabolites **1**−**8**.

RESULTS AND DISCUSSION

The NMR data for palmarumycins BG1−7 (**1**−**7**) suggested that they were new members of natural metabolites in the palmarumycins family.[4,5] The common structural feature of palmarumycins **1**−**7** is the 1,8-dioxynaphthalene moiety linked to a decalin unit via a spiroketal carbon resonating at approximately 100 ppm in the ^{13}C NMR spectrum. NMR spectroscopic data of the dioxynaphthalene moiety and the bridging carbon atom of all the seven compounds were virtually the same. Thus, the structure elucidation of palmarumycins BG1−7 (**1**−**7**) focused mainly on establishing the remaining portions of the molecules, especially the relative configuration in those having multiple chirality centers as well as the absolute configuration by CD analysis.

Palmarumycin BG1 (**1**) was isolated as a yellow powder. The molecular formula of palmarumycin BG1 (**1**) was determined to be $C_{20}H_{14}O_5$ (14 degrees of unsaturation) by HRESIMS analysis (*m*/*z* 357.0737 [M + Na]$^+$, calcd, 357.0739), which was supported by the ^{1}H and ^{13}C NMR data (see Tables 1 and 2). Its IR absorptions implied the presence of hydroxyl (3432 cm^{-1}) and ketone carbonyl (1641 cm^{-1}) functionalities. Apart from a set of NMR signal characteristic of the dioxynaphthalene moiety, the ^{1}H and ^{13}C NMR spectra showed signals for a 1,2,3-trisubstituted aromatic ring,

Received: December 22, 2010
Published: February 18, 2011

Table 1. ^{1}H NMR Data [δ_H (mult; $^3J_{H,H}$)] for Compounds 1−8[a] (2−8; 300 MHz)

proton	1[b](400 MHz)	2[b]	3[c]	4[c]	5[b]	6[b]	7[c]	8[b]
1		5.01 (d, 5.1)	5.25 (dd, 8.7, 6.0)	5.43 (dd, 5.1, 4.8)	5.39 (d, 9.0)	5.33 (dd, 7.8, 4.5)	5.35 (d, 8.1)	
OH-1					3.7 (s)			
2β	2.94 (dd, 18.0, 4.0)	2.41 (ddd, 15.3, 1.8, 1.2)	2.22 (ddd, 13.5, 9.0, 2.1)	2.22 (ddd, 13.8, 4.8, 3.0)	4.66 (dd, 9.0, 1.8)	4.63 (dd, 8.7, 7.8)	4.56 (dd, 8.1, 2.1)	3.03 (dd, 18.3, 2.4)
2α	3.24 (dd, 18.0, 4.0)	2.52 (ddd, 15.3, 5.1, 3.3)	2.38 (m)	2.53 (m)				3.45 (dd, 18.0, 3.0)
3	4.59 (t, 4.0)	4.42 (d, 3.3)	4.26 (dd, 5.7, 2.1)	4.53 (dd, 9.6, 3.0)	4.44 (d, 1.8)	4.38 (dd, 8.7, 4.5)	4.23 (d, 2.1)	4.69 (dd, 3.0, 2.4)
OH-3	2.41 (brs)				2.66 (s)			
6	7.34 (d, 8.0)	7.44 (d, 8.1)	7.15 (d, 8.4)	7.30 (dd, 8.1, 1.5)	7.41 (dd, 8.1, 1.5)	7.03 (d, 7.8)	7.63 (dd, 8.4, 1.5)	
7	7.53 (t, 8.0)	7.39 (dd, 8.1, 7.8,)	7.15 (t, 8.4)	7.24 (dd, 8.1, 7.8)	7.36 (dd, 8.1, 7.5)	7.18 (dd, 8.1, 7.8)	7.45 (dd, 8.4, 7.5)	7.04 (d, 9.0)
8	7.08 (d, 8.4)	7.08 (dd, 7.8, 1.8)	6.84 (d, 8.4)	7.56 (dd, 7.8, 1.2)	7.02 (dd, 7.5, 1.5)	6.96 (d, 8.1)	7.71 (dd, 8.1, 1.2)	6.94 (d, 9.0)
OH-9	12.36 (brs)				8.51 (s)	8.15 (s)		11.59 (s)
1′	7.56 (d, 8.0)	7.65 (d, 8.7)	7.46 (d, 8.1)	7.46 (dd, 8.1, 1.5)	7.53 (d, 8.1)	7.49 (d, 7.2)	7.57 (d, 8.1)	
2′β	7.49 (dd, 8.0, 7.6)	7.49 (dd, 8.7, 7.8)	7.40 (dd, 8.1, 7.2)	7.42 (dd, 8.1, 7.2)	7.47 (dd, 8.1, 7.5)	7.41 (dd, 8.4, 7.2)	7.46 (dd, 8.1, 7.8)	2.89 (ddd, 17.4, 6.0, 1.5)
2′α								3.30 (m)
3′β	7.08 (d, 7.6)	7.05 (d, 7.8)	6.90 (d, 6.9)	6.92 (dd, 7.2, 1.5)	6.89 (d, 6.9)	6.96 (d, 8.1)	6.93 (d, 7.5)	2.48 (m)
3′α								2.78 (ddd,12.9, 6.0, 1.5)
7′	6.91 (d, 7.6)	6.87 (d, 7.5)	6.81 (d, 7.5)	6.85 (dd,7.5, 1.5)	7.07 (d, 7.2)	6.90 (d, 7.2)	7.07 (d, 7.2)	7.08 (d, 8.4)
8′	7.44 (dd, 8.4, 7.6)	7.42 (dd, 8.1, 7.5)	7.37 (dd, 7.5, 7.2)	7.42 (dd, 8.1, 7.5)	7.43 (dd, 8.1, 7.5)	7.45 (dd, 8.7, 7.2)	7.5 (dd, 7.5, 7.2)	7.41 (dd, 8.1, 8.1)
9′	7.54 (d, 8.4)	7.55 (d, 8.1)	7.44 (d, 7.2)	7.46 (dd, 8.1, 1.5)	7.56 (d, 8.1)	7.49 (d, 8.4)	7.57 (d, 8.7)	7.65 (dd, 7.5, 0.9)

[a] The assignments were based on DEPT, ^{1}H−^{1}H COSY, HSQC, and HMBC experiments. [b] Spectrum taken in $CDCl_3$. [c] Spectrum taken in CD_3OD.

dx.doi.org/10.1021/jo1024877 | J. Org. Chem. 2011, 76, 1821–1830

Table 2. ^{13}C NMR Data (100 MHz) for Compounds 1−8[a]

carbon	1[b]	2[b]	3[c]	4[c]	5[b]	6[b]	7[c]	8[b]
1	201.0 (C)	63.1 (CH)	65.7 (CH)	63.8 (CH)	71.3 (CH)	73.5 (CH)	72.2 (CH)	199.9 (C)
2	41.2 (CH_2)	31.6 (CH_2)	36.6 (CH_2)	36.5 (CH_2)	63.6 (CH)	64.2 (CH)	65.0 (CH)	41.1 (CH_2)
3	67.1 (CH)	65.5 (CH)	68.1 (CH)	69.7 (CH)	70.6 (CH)	74.4 (CH)	71.5 (CH)	70.0 (CH)
4	98.6 (C)	99.5 (C)	101.2 (C)	101.4 (C)	99.5 (C)	99.1 (C)	101.8 (C)	93.9 (C)
5	137.8 (C)	131.9 (C)	136.4 (C)	138.4 (C)	132.4 (C)	133.9 (C)	135.3 (C)	112.8 (C)
6	117.9 (CH)	119.5 (CH)	120.3 (CH)	125.2 (CH)	119.7 (CH)	118.3 (CH)	125.2 (CH)	143.0 (C)
7	137.1 (CH)	130.2 (CH)	130.5 (CH)	130.4 (CH)	130.6 (CH)	130.4 (CH)	130.6 (CH)	126.0 (CH)
8	119.8 (CH)	118.0 (CH)	118.0 (CH)	124.8 (CH)	118.8 (CH)	118.7 (CH)	124.7 (CH)	121.1 (CH)
9	162.0 (C)	155.3 (C)	157.7 (C)	152.5 (C)	155.5 (C)	155.9 (C)	152.7 (C)	157.1 (C)
10	115.2 (C)	124.6 (C)	126.9 (C)	133.3 (C)	120.2 (C)	119.0 (C)	132.5 (C)	117.0 (C)
1′	121.4 (CH)	121.2 (CH)	121.9 (CH)	121.5 (CH)	121.0 (CH)	120.6 (CH)	122.4 (CH)	195.5 (C)
2′	127.7 (CH)	127.7 (CH)	129.2 (CH)	128.9 (CH)	127.6 (CH)	127.5 (CH)	129.1 (CH)	33.6 (CH_2)
3′	109.5 (CH)	109.3 (CH)	111.0 (CH)	109.3 (CH)	109.1 (CH)	108.3 (CH)	110.3 (CH)	32.7 (CH_2)
4′	146.2 (C)	146.8 (C)	149.2 (C)	150.6 (C)	146.1 (C)	146.9 (C)	149.1 (C)	93.4 (C)
5′	113.0 (C)	113.3 (C)	115.2 (C)	114.7 (C)	113.0 (C)	112.6 (C)	115.1 (C)	122.5 (C)
6′	147.0 (C)	147.1 (C)	149.9 (C)	149.5 (C)	146.8 (C)	147.9 (C)	148.8 (C)	148.8 (C)
7′	108.8 (CH)	108.9 (CH)	109.7 (CH)	110.2 (CH)	109.6 (CH)	108.6 (CH)	111.5 (CH)	121.5 (CH)
8′	127.6 (CH)	127.5 (CH)	128.9 (CH)	129.1 (CH)	127.6 (CH)	127.5 (CH)	129.3 (CH)	131.0 (CH)
9′	121.1 (CH)	120.8 (CH)	121.8 (CH)	121.5 (CH)	121.5 (CH)	120.8 (CH)	122.4 (CH)	120.9 (CH)
10′	134.1 (C)	134.1 (C)	136.0 (C)	135.9 (C)	134.1 (C)	133.9 (C)	136.1 (C)	130.9 (C)

[a] The assignments were based on DEPT, ^{1}H−^{1}H COSY, HSQC, and HMBC experiments. [b] Spectrum taken in $CDCl_3$. [c] Spectrum taken in CD_3OD.

a ketal carbon, a ketone moiety, one oxymethine, one methylene, and two hydroxyl groups [one of which is highly chelated (δ_H 12.36)]. The connectivities among these units were determined by the analysis of ^{1}H−^{1}H COSY and HMBC spectra. Analysis of the COSY NMR data led to the identification of two isolated proton spin systems corresponding to the C-2−C-3 and C-6−C-8 subunits of structure **1**. HMBC correlations of H-2 and H-3 with carbonyl C-1 and ketal carbon C-4, H-2 with C-10, and H-3 with C-5 led to the assignment of the nonaromatic ring. Correlation of H-6 to C-1, C-4, C-5 and C-10, H-8 to C-9 and C-10, and OH-9 (δ_H 12.36, brs) to the carbonyl carbon C-1 enabled the connection of the C-5 and C-9 of the aromatic ring to C-4 and C-10 respectively, resulting in a tetralone moiety. The dioxynaphthalene unit must be linked to C-4 via two oxygen atoms of the ketal moiety, thereby completing the planar structure of **1** as shown in Scheme 1.

In palmarumycin BG1 (**1**), the axial orientation of the hydroxyl group at C-3 was concluded from the small coupling constants observed between H-2s and H-3 ($^3J_{2H,3H}$ = 4.0 Hz), which was also independently confirmed by the MMFF conformational search followed by TDDFT optimization at the B3LYP/6-31G(d) level. The conformational analysis of (3*R*)-**1** found the *M* helicity conformer with 3-OH_{ax} the lowest energy one with 95.5% population, which is probably due to the hydrogen bonding of the 3-OH_{ax} to one of the acetal oxygens (Figure 1). This hydrogen bonding would not be feasible in the *P* helicity conformer having an equatorial 3-OH. The chiroptical properties of palmarumycin BG1 (**1**) are governed by both its central chirality element (absolute configuration of C-3) and the conformation (helicity of fused nonaromatic ring), although these two are intertwined. In the lowest energy conformer, the nonaromatic ring adopts an envelop conformation of *M* helicity with torsional angle $\omega_{C5,C4,C3,C2}$ = −53.1, which also defines the relative orientation of the aryl and phenyl chromophores. The CD spectrum of **1** showed an intense negative couplet around 220 nm [226 nm ($\Delta\varepsilon$ = −54.9), 209 (22.91)] and negative Cotton effects (CEs) at 251 and 328 nm accompanied with a negative

Scheme 1. Compounds 1−8 Isolated from the Mangrove *Bruguiera gymnorrhiza*

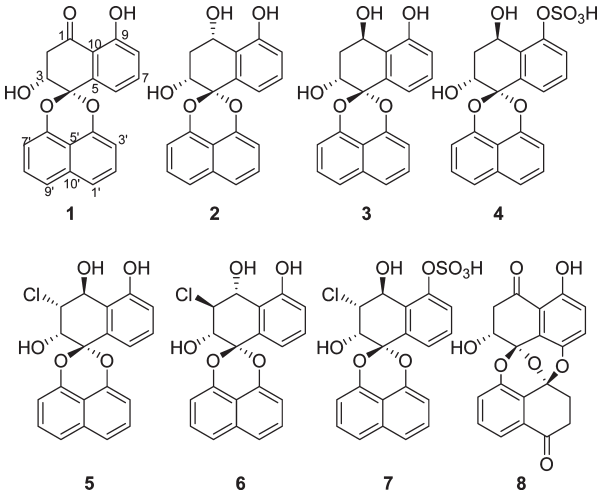

plateau. It is noteworthy that the tetralone n−π^* transition above 300 nm is overlapped by the naphthalene ^1L_b band making its application ambiguous for the determination of absolute configuration. The CD spectra calculated for the (3*R*) enantiomer of the lowest energy conformer (95.5% population) with various functionals (B3LYP, BH&HLYP, CAM-B3LYP) and TZVP basis set reproduced well the experimental CD, with B3LYP/TZVP giving the best agreement (Figure 2). Thus, the absolute configuration could be unambiguously determined as 3*R*, which is in keeping with the opposite specific rotation value of the known enantiomeric (3*S*)-palmarumycin JC2.[19−22]

Compound **2** (palmarumycin BG2) was isolated as a white solid. An HREIMS analysis gave a molecular ion at *m*/*z*

dx.doi.org/10.1021/jo1024877 |*J. Org. Chem.* 2011, 76, 1821–1830

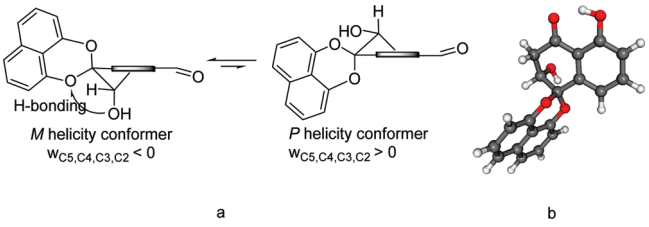

Figure 1. (a) Two equilibrating *M* and *P* helicity conformers of (3*R*)-palmarumycin BG1 [(3*R*)-**1**] viewed from the direction of the benzene ring and definition of helicity of the fused nonaromatic ring of the tetralone chromophore. Thick line represents the benzene ring. (b) DFT-optimized geometry of the lowest energy conformer (95.5% population) of (3*R*)-**1**.

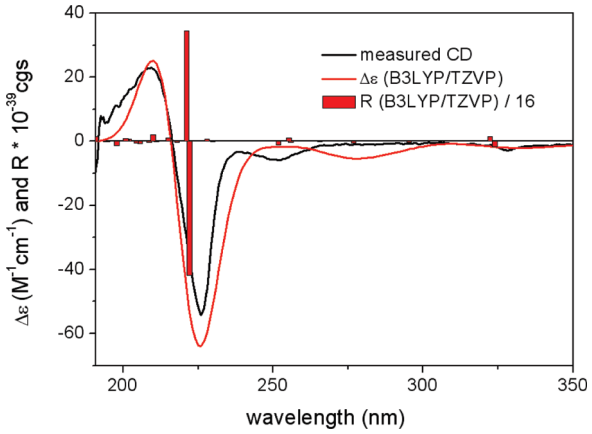

Figure 2. Experimental CD spectrum of (3*R*)-**1** in methanol compared with the B3LYP/TZVP spectrum calculated for the (3*R*) enantiomer of the lowest energy conformer having *M* helicity and an axial 3-OH group.

336.0998, which was consistent with the molecular formula $C_{20}H_{16}O_5$, indicating 13 degrees of unsaturation. Two additional hydrogens in the molecular formula relative to that of **1** and analysis of the ^{1}H and ^{13}C NMR spectrum revealed that the carbonyl carbon of **1** was reduced to a hydroxyl group in **2**. This has also been supported by the disappearance of the highly chelated hydroxyl group in **2**. The ^{1}H−^{1}H COSY spectra also clearly showed a correlation between these H-1 (δ_H 5.01, d, J = 5.1 Hz) and H-2eq (δ_H 2.52, ddd, J = 15.3, 5.1, 3.3 Hz). Proton and carbon chemical shift assignments were made by analysis of HSQC and HMBC experiments. The *cis* relative configuration of **2** was proposed on the ground of the $^3J_{H,H}$ coupling constants. The small $^3J_{1H,2H}$ coupling constants (5.1 Hz) indicated that H-1 must adopt a *pseudoequatorial* orientation with a half-chair conformation of the six-membered ring, while the coupling constants of the 3-H ($^3J_{2H,3Heq}$= 3.3 Hz) proved that the 3-OH group is axially oriented. The MMFF conformational search followed by DFT optimization also confirmed that the lowest-energy conformer of (1*S*,3*R*)-palmarumycin BG2 has *M* helicity with axial 1- and 3-OH groups (Figure 3) with high population (99.9%). The unexpectedly exclusive population of the diaxial conformer can be explained by the hydrogen bonding of the 3-OH to the acetal oxygen and the decrease of the *peri* interaction between the axial 1-OH and the phenolic 9-OH. The experimental CD curve of palmarumycin BG2 was quite similar to that of **1** with negative couplet around 220 nm and negative plateau between 250 and 330 nm. All the three DFT calculated CD spectra (B3LYP, BH&HLYP, CAM-B3LYP) of (1*S*,3*R*)-**2** showed a good agreement with the experimental CD affording the determination of its absolute configuration as (−)-(1*S*,3*R*)-palmarumycin BG2 (Figure 4).

Palmarumycin BG3 (**3**) was assigned to the same molecular formula $C_{20}H_{16}O_5$ as palmarumycin BG2 (**2**) on the basis of HRESIMS analysis (m/z 359.0915 $[M + Na]^+$, calcd, 359.0895) and NMR data (Tables 1 and 2). Compound **3** was obtained as a white solid, and it showed poor solubility in $CHCl_3$ but good solubility in MeOH and acetone, behavior which was different from that of compound **2**. Detailed analysis of NMR data revealed that compound **3** is the C-1 epimer of compound **2**; i.e., it has *trans* relative configuration. The large $^3J_{1H,2Hax}$ (8.7 Hz) and the small $^3J_{2H,3Heq}$ (5.7 and 2.1 Hz) coupling constants indicated that 1-OH and 3-H must adopt a *pseudoaxial* orientation. The result of the conformational analysis was in full accordance with the NMR findings, since the 1-OH_{eq}, 3-OH_{ax} conformer with *M* helicity was obtained as the lowest energy conformer with 89.2% population (see Figure S1 in the Supporting Information). Thus, the epimerization at C-1 did not invert the conformation of the fused nonaromatic ring; it preserved its *M* helicity indicating the importance of the stabilizing affect of the hydrogen bonding of the axial 3-OH group on the preferred conformation. Since both the helicity and relative arrangement of the naphthyl and phenyl chromophores remained the same as in (−)-(1*S*,3*R*)-palmarumycin BG2, the CD spectrum also showed great similarity. The DFT-calculated spectra (B3LYP, BH&HLYP, CAM-B3LYP) of (1*R*,3*R*)-**3** were nearly identical with the experimental CD curve (Figure 5, B3LYP/TZVP results shown), which allowed determination of the absolute configuration as (−)-(1*R*,3*R*)-palmarumycin BG3.

Palmarumycin BG4 (**4**) was isolated as a white solid and was the most polar compound among palmarumycins BG1−7. The HRESIMS of **4** showed a major ion peak at m/z 415.0476 $[M - H]^-$, corresponding to the molecular formula $C_{20}H_{16}O_8S$ (calcd for $C_{20}H_{15}O_8S$, 415.0488), suggesting the presence of a sulfate group in the molecule. The LRESIMS of **4** gave the highest mass ion peak at m/z 415, which was assigned to the $[M - H]^-$ ion. Moreover, the MS/MS analysis of the ion at m/z 415 showed an ion peak at m/z 335 $[M - H - 80]^-$, corresponding to the loss of a sulfate group, which was consistent with the presence of a sulfate group in the molecule. Detailed analysis of NMR data revealed that compound **4** has the same planar structure as compound **2**, but the substitution pattern of the aromatic ring was different. The ^{13}C NMR data showed significant changes in chemical shifts of the aromatic ring relative to those of **2**. The upfield shift observed for C-9 (δ_C 152.5) and downfield shift observed for C-8 (δ_C 124.8) and C-10 (δ_C 133.3) suggested the presence of sulfate group at C-9. HMBC correlation of H-1, H-7, and H-8 to C-9 further confirmed the position of the sulfate group at C-9. The relative configuration of compound **4** was established by the analysis of ^{1}H−^{1}H NMR coupling constants, NOESY data and by comparison of its ^{1}H NMR data with those of palmarumycin BG2 (**2**). The large $^3J_{2Hax,3H}$ coupling constant (9.6 Hz) indicated that 3-OH must adopt an equatorial orientation, while the $^3J_{1H,2H}$ coupling constants (5.1 and 4.8 Hz) suggested that 1-OH is axially oriented. This implies that **4** has also a *trans* relative configuration such as **3** but a different conformation from that of **3**, in which the 1-OH is equatorial and the 3-OH is axial. The different conformation of **4** is presumably due to the presence of the 9-sulfoxy group, which pushes the 1-OH to an axial position to reduce the *peri* interaction. The MMFF conformational search followed by DFT optimization with implicit solvent model afforded four conformers, from which the two lowest energy ones (53.1% and 24.1% populations) have 1-OH_{eq}−3-OH_{ax} conformation, while the other two (12.2% and 10.6% populations) have 1-OH_{ax}−3-OH_{eq}

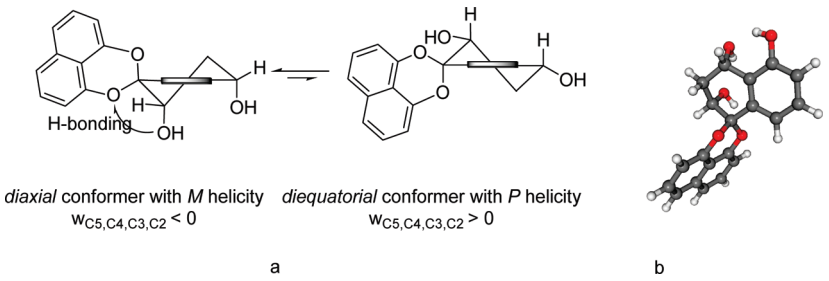

Figure 3. (a) Two equilibrating *M* and *P* helicity conformers of (1*S*, 3*R*)-palmarumycin BG2 [(1*S*, 3*R*)-**2**]. (b) DFT optimized geometry of the most stable conformer (99.9%) of (1*S*,3*R*)-**2**.

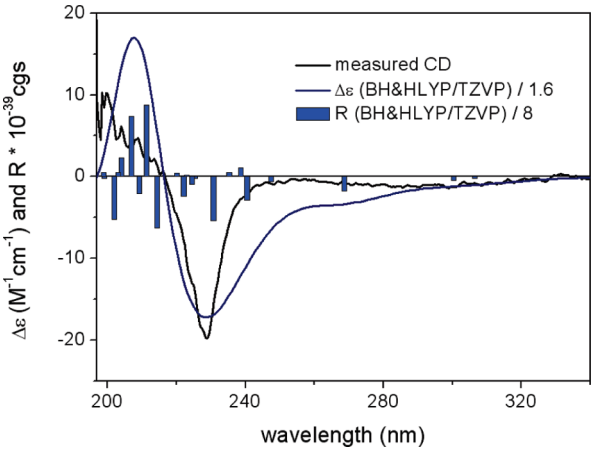

Figure 4. Experimental CD spectrum of (1*S*,3*R*)-**2** in methanol, compared with the BH&HLYP/TZVP spectrum calculated for the (1*S*,3*R*) enantiomer of the lowest-energy conformer having *M* helicity.

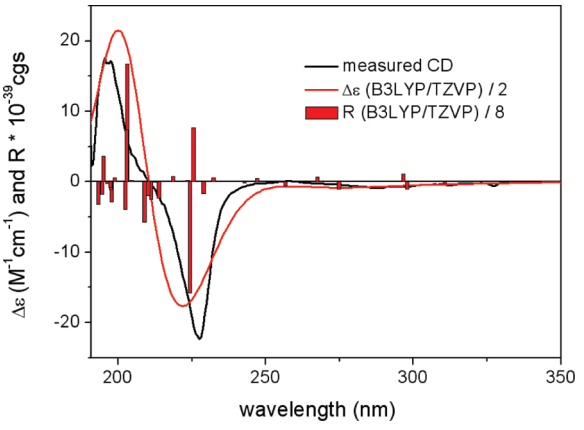

Figure 5. Experimental CD spectrum of (1*R*,3*R*)-**3** in methanol compared with the B3LYP/TZVP spectrum calculated for the (1*R*,3*R*) enantiomer of the lowest energy enantiomer (89.2% population).

conformation (see the Figure S2 in the Supporting Information). Thus the result of the conformational analysis does not corroborate the $^3J_{H,H}$ coupling constants, which suggests that the 1-OH_{ax}−3-OH_{eq} conformers should be the major ones. The experimental CD spectrum was then compared with the CD spectrum calculated for the 1-OH_{ax}−3-OH_{eq} conformers of (1*S*,3*S*)-**4** instead of the Boltzmann-weighted average CD of all the computed conformers (Figure 6). On the basis of the experimental 211 nm CD band ($\Delta\varepsilon = 11.78$), the mirror image of which was reproduced by the CD calculation of (1*S*,3*S*)-**4**, the absolute configuration of (+)-**4** can be assigned as (1*R*,3*R*). However, it has to be noted that the low energy CD transitions could not reproduce well by the CD spectrum calculated for the 1-OH_{ax}−3-OH_{eq} conformers of (1*S*,3*S*)-**4**. Thus, (−)-**3** and (+)-**4** are homochiral, but they have markedly different CD spectra and specific rotations of opposite signs, which can be attributed to the opposite helicity of their fused nonaromatic rings. The nonaromatic ring of the decalin chromophore has *M* helicity in (−)-(1*R*,3*R*)-**3** and *P* helicity in (+)-(1*R*,3*R*)-**4**, which explains their different optical parameters (Figure 7).

Palmarumycin BG5 (**5**) was isolated as a brown solid. A HRESIMS analysis gave a molecular ion at *m*/*z* 393.0521$[M + Na]^+$, which was consistent with the molecular formula $C_{20}H_{15}O_5Cl$, indicating 14 degrees of unsaturation. One additional chlorine atom and one missing hydrogen in the molecular formula compared to that of **3**, and analysis of the ^1H and ^{13}C NMR spectrum indicated that compound **5** is a monochloro derivative. This was consistent with the EIMS data, which showed peaks for $[M]^+$ and $[M + 2]^+$ in a ratio of 3:1 due to the chlorine isotope. A detailed analysis of ^1H and ^{13}C NMR data for **5** (Tables 1 and 2) indicated that signal for the methylene (δ_H 2.38, 2.22; δ_C 36.6, C-2) in **3** was replaced by a methine (δ_H 4.66; δ_C 63.6, C-2) in the NMR spectra of **5**. On the basis of these data, the position of the chlorine atom was assigned at C-2 in compound **5**. The $^1H-^1H$ COSY and HMBC correlations among the C-1−C-3 subunit also confirmed this conclusion. ^1H and ^{13}C NMR assignments were made by analysis of HSQC and HMBC data. The relative configuration of palmarumycin BG5 (**5**) was proposed as shown in Scheme 1 by the analysis of $^1H-^1H$ coupling constants and NOESY data. The large $^3J_{1Hax,2Hax}$ (9.0 Hz) and the small $^3J_{2Hax,3Heq}$ (1.8 Hz) coupling constants indicated that H-1 and H-2 must adopt axial orientations, while H-3 has an equatorial orientation implying a 1,2-*trans*, 3,4-*cis* relative configuration. In accordance with the observed coupling constants, the conformational analysis found the *M* helicity (1-OH_{eq}, 2-Cl_{eq}, 3-OH_{ax}) conformer of (1*S*,2*R*,3*S*)-palmarumycin BG5 (**5**) to be the most abundant one with 91.7% population (Figure 9). The CD spectrum also showed a negative CD couplet around 220 nm [227 nm ($\Delta\varepsilon = -42.74$), 194 (27.34)] and negative CEs above 240 nm, which could be reproduced well by the DFT CD calculations performed on the (1*S*,2*R*,3*S*) enantiomer (Figure 8). Thus the absolute configuration of palmarumycin BG5 (**5**) could be determined as (−)-(1*S*,2*R*,3*S*).

Palmarumycin BG6 (**6**) was assigned to have the same molecular formula $C_{20}H_{15}O_5Cl$ as palmarumycin BG5 (**5**) on the basis of HRESIMS analysis (*m*/*z* 393.0508 $[M + Na]^+$, calcd 393.0506) and NMR data (Tables 1 and 2). Compound **6** was isolated as a brown solid, and it was more polar than compound **5**.

dx.doi.org/10.1021/jo1024877 |*J. Org. Chem.* 2011, 76, 1821–1830

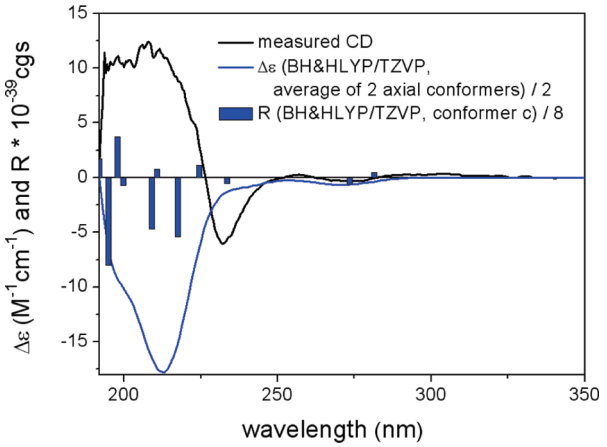

Figure 6. Measured CD spectrum of (1*R*,3*R*)-**4** in methanol compared with the BH&HLYP/TZVP spectrum calculated for the two 1-OH_{ax} conformers of (1*S*,3*S*)-**4**.

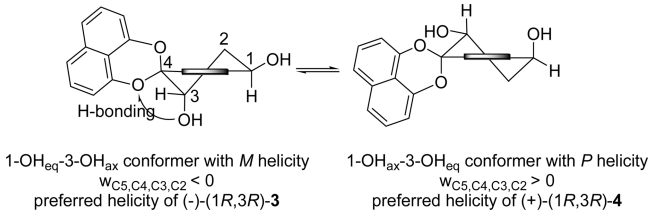

Figure 7. Equilibrating *M* and *P* helicity conformers of (1*R*,3*R*)-palmarumycin BG3 (**3**) [(1*R*,3*R*)-**3**] and (1*R*,3*R*)-palmarumycin BG4 (**4**).

A detailed analysis of the NMR data indicated that compound **6** has the same planar structure as compound **5**. The 1,2-*trans*, 3,4-*trans* relative configuration of compound **6** was proposed on the basis of $^{1}H-^{1}H$ coupling constants. The $^{3}J_{H,H}$ coupling constants ($^{3}J_{1H,3H}$ = 4.5 Hz, $^{3}J_{2H,3H}$ = 8.7 Hz) indicated that 1-H, 2-H, and 3-H adopt *trans-pseudoaxial* orientations and **6** differs in the 3,4-*trans* orientation from **5**. The *cis*-1,3-diaxial orientation of 1-H and 3-H was also confirmed by the observed NOE effect between these two protons. In contrast, the conformational analysis of **6** surprisingly showed that the lowest energy conformer is the all axial conformer (conformer a, see Figure S3 in the Supporting Information) with 50% population, in which the 1- and 3-OHs and the 2-Cl have axial orientation and the 3-OH is hydrogen bonded to one of the acetal oxygens. The all-equatorial geometry with equatorial 1- and 3-OHs and the 2-Cl is represented by three slightly different conformers totaling a population of 39.4%. Moreover, two minor conformers with a boat conformation of the fused nonaromatic ring were also calculated with 10.5% overall population. Thus, the conformational analysis result was clearly not in accordance with the NMR results, which showed that the all-equatorial conformer(s) is the major one in solution. The measured CD spectrum of **6** showed CEs opposite to the those of (1*S*,2*R*,3*S*)-**5** in nearly the whole CD spectrum, although their CD spectra were far from being mirror image ones (Figure 10). The CD spectrum obtained as the Boltzmann-weighted average of the calculated solution conformers of (1*S*,2*R*,3*R*)-**6** did not reproduce the experimental CD curve (Figure S4, Supporting Information). On the basis of the NMR results, only the all-equatorial conformers of (1*S*,2*R*,3*R*)-**6** were then considered for CD calculation, which gave nearly identical CD spectra and mirror image curves with the experimental

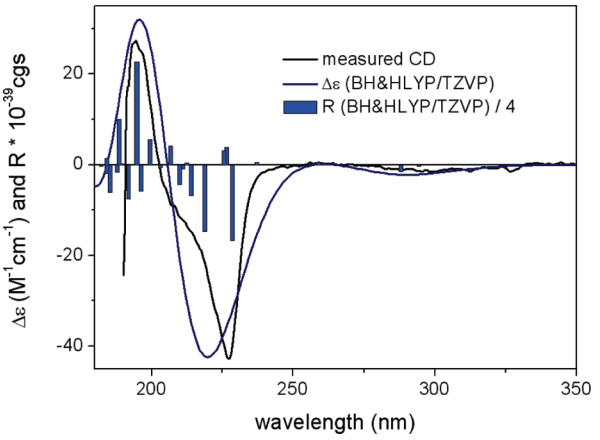

Figure 8. Measured CD spectrum of (1*S*,2*R*,3*S*)-**5** in methanol compared with the BH&HLYP/TZVP spectrum calculated for the (1*S*,2*R*,3*S*) enantiomer of the lowest-energy conformer of **5**.

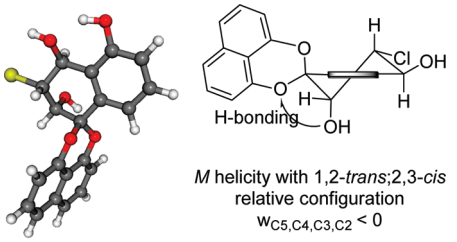

Figure 9. DFT-optimized geometry and helicity of the most stable conformer (91.7%) of **5**.

CD spectrum (Figure 10). This confirmed unambiguously that it is indeed the all-equatorial conformer that is the major one in solution determining the chiroptical properties, and thus, the absolute configuration of **6** was assigned as (+)-(1*R*,2*S*,3*S*). With (1*R*,2*S*,3*S*) absolute configuration and equatorial orientation of 1- and 3-OHs and 2-Cl, the fused nonaromatic ring of **6** adopts *P* helicity, opposite to the *M* helicity of (1*S*,2*R*,3*S*)-**5**, which explains their opposite CEs in their CD spectra.

Palmarumycin BG7 (**7**) was isolated as a brown solid. The molecular formula was determined as $C_{20}H_{15}O_8SCl$ (14 degrees of unsaturation) by HRESIMS in negative-ion mode, which showed a deprotonated parent ion peak at *m*/*z* 449.0097 $[M - H]^-$ (calcd 449.0098). The ESIMS of **7** gave the ion peak at *m*/*z* 449/451 (in a ratio of 3:1), which was assigned to the $[M - H]^-$ ion. The MS/MS analysis of the ion at *m*/*z* 449 $[M - H]^-$ showed an ion peak at *m*/*z* 415 $[M - 35]^-$ corresponding to the loss of a chlorine atom. A further ion peak was also observed at *m*/*z* 371 $[M - H - 80]^-$, corresponding to the loss of a sulfate group. Detailed analysis of MS and NMR data of compound **7** suggested that palmarumycin BG7 (**7**) is the sulfoxy derivative of compound **5**. The assignment of the position of the sulfoxy group (C-9) is mainly based on chemical shift and HMBC data in comparison with those of palmarumycin BG5 (**5**). ^{1}H and ^{13}C NMR assignments were made by the analysis of HSQC and HMBC data. The relative configuration of **7** was determined to be the same as that of **5** by analysis of $^{1}H-^{1}H$ coupling constants and NOESY data. Since **7** showed similar coupling constant pattern and CD those of spectra to (−)-(1*S*,2*R*,3*S*)-**5**, its absolute configuration was determined as (−)-(1*S*,2*R*,3*S*)-**7**. It is noteworthy that in contrast to **3** and its sulfonated derivative **4**, the fused nonaromatic ring of both **5** and **7** have *M* helicity; i.e., the

dx.doi.org/10.1021/jo1024877 |*J. Org. Chem.* 2011, 76, 1821–1830

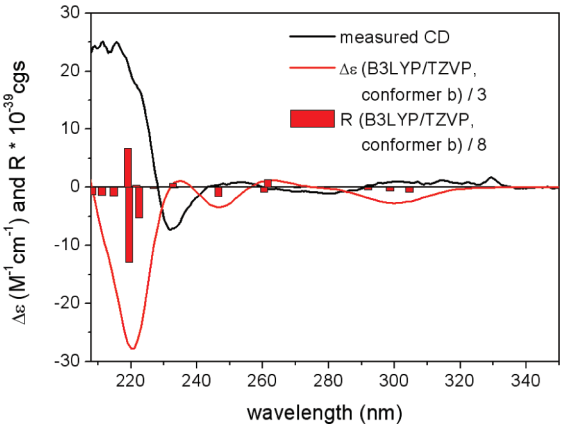

Figure 10. Experimental CD spectrum of (1*R*,2*S*,3*S*)-**6** in MeOH compared with the B3LYP/TZVP spectrum calculated for conformer b (1-OH_{eq}, 2-Cl_{eq}, 3-OH_{eq}; see the Supporting Information for geometry) of the (1*S*,2*R*,3*R*)-enantiomer.

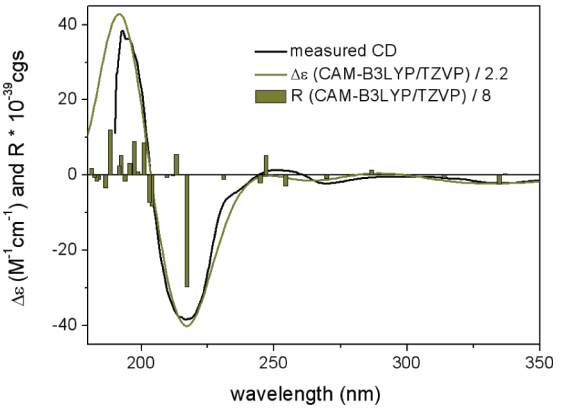

Figure 11. Experimental CD spectrum of (3*R*,4*S*,4′*R*)-**8** in methanol compared with the CAM-B3LYP/TZVP spectrum calculated for the (3*R*,4*S*,4′*R*) enantiomer of the lowest energy conformer.

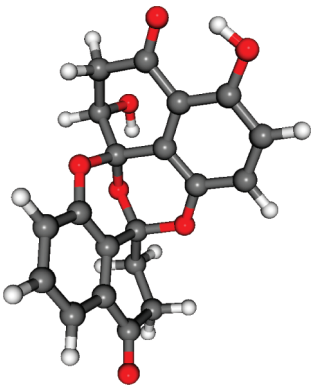

Figure 12. DFT-optimized geometry of the most stable conformer (99.7%) of (3*R*,4*S*,4′*R*)-**8**.

introduction of a 9-sulfoxy group did not induce a conformational change in **7**.

Preussomerin BG1 (**8**) was obtained as a yellow solid. HREIMS analysis of preussomerin BG1 (**8**) gave a molecular ion at *m*/*z* 366.0742 (calcd 366.0740) that determined the molecular formula as $C_{20}H_{14}O_7$, and this conclusion was supported by the ^{1}H and ^{13}C NMR data. Compound **8** had characteristic bis-spiro-bisnaphthalene NMR signals due to an oxygenated 1,2,3,4-tetrasubstituted aromatic ring [δ_H 6.94 (d, *J* = 9.0 Hz, H-8) and 7.04 (d, *J* = 9.0 Hz, H-7); δ_C 112.8 (C-5), 143.0 (C-6), 126.0 (C-7), 121.1 (C-8), 157.1 (C-9), and 117.0 (C-10)], an oxygenated 1,2,3-trisubsituted aromatic ring [δ_H 7.08 (d, *J* = 8.4 Hz, H-7′), 7.41 (t, *J* = 8.1 Hz, H-8′), and 7.65 (dd, *J* = 7.5, 0.9 Hz, H-9′); δ_C 122.5 (C-5′), 148.8 (C-6′), 121.5 (C-7′), 131.0 (C-8′), 120.9 (C-9′), and 130.9 (C-10′)], a highly chelated phenolic OH group [δ_H 11.59 (C-9)], and two spiroketal quaternary carbons [δ_C 93.9 (C-4); 93.4 (C-4′)]. In addition, the ^{1}H and ^{13}C NMR spectrum showed signals for two carbonyl carbons [δ_C 199.9 (C-1); 195.5 (C-1′)], three methylenes [δ_H 3.03 (dd, *J* = 18.3, 2.4 Hz, H-2β), 3.45 (dd, *J* = 18.0, 3.0 Hz, H-2α), 2.89 (ddd, *J* = 17.4, 6.0, 1.5 Hz, H-2′β), 3.30 (m, H-2′α), 2.48 (m, H-3′β), 2.78 (ddd, *J* = 12.9, 6.0, 1.5 Hz, H-3′α)], and one oxygenated methine [δ_H 4.69 (t, *J* = 3.0, H-3)]. Analysis of the COSY and HMBC NMR data led to the identification of two isolated proton spin-systems corresponding to the C-1−C-3 and C-1′−C-3′ subunits of **8**. HMBC correlations of H-2 to the carbonyl C-1, the ketal C-4 and C-5, and H-3 to C-1 and C-4 confirmed that C-1 and C-3 were attached to C-10 and C-4, respectively, while C-1′ and C-3′ were bonded to C-10′ and C-4′, respectively on the basis of correlation of H-9′ with C-1′, H-3′ with C-1′ and C-5′, and H-2′ with C-1′ and C-10′. The small $^3J_{2H,3H}$ coupling constants (3.0 and 2.4 Hz) indicated that H-3 adopts a pseudoequatorial orientation at C-3. On the basis of NMR spectroscopic data, the structure of preussomerine BG1 (**8**) was established as depicted in Scheme 1. Although this is the first report of compound **8** as a natural product, Singh and co-workers in 1994 described the synthesis of **8** by means of palladium-catalyzed hydrogenation of preussomerin G in ethyl acetate. The ^{1}H NMR data of compound **8** were fully consistent with the reported values of the synthetic derivative.[6] The conformational analysis of **8** afforded a single solution conformer with 99.7% population, in which the 3-OH is axial and hydrogen bonded to one of the ketal oxygens (Figure 12). The CD spectra calculated for the (3*R*,4*S*,4′*R*) enantiomer with B3LYP, BH&HLYP, and CAM-B3LYP methods reproduced very well the experimental spectrum in the full spectral range with CAM-B3LYP/TZVP giving the best agreement (Figure 11). Thus the absolute configuration of palmarumycin BG8 was unambiguously determined as (−)-(3*R*,4*S*,4′*R*). The (−)-(3*R*,4*S*,4′*R*) absolute configuration and CD data of **8** corroborates the CD data of preussomerin L, which differs from **8** in the presence of an additional hydroxyl group at the C-3′ position.[23]

The cytotoxic activities of **1**−**8** against the growth of tumor cell lines (MCF-7 and HL 60) were evaluated. The results indicated that palmarumycin BG5 (**5**) exhibited cytotoxicity against human breast carcinoma MCF-7 (IC_{50} 7.6 μM) and human promyelocytic leukemia HL 60 (IC_{50} 1.9 and 3.1 μM, respectively). Unfortunately, other compounds were inactive against the above cancer cells.

CONCLUSION

Eight novel spirodioxynaphthalenes, palmarumycins BG1−7 (**1**−**7**) and preussomerin BG1 (**8**), were isolated from the mangrove *B. gymnorrhiza*. Among them, compounds **4** and **7** are new members of the so-called spirodioxynaphthalene class with a sulfate group which is unprecedented among the compounds of this class. Moreover, it is interesting to note that the hydroxyl groups at C-3 in **1**−**8** have always α orientation, although their Cahn−Ingold−Prelog notations are different

dx.doi.org/10.1021/jo1024877 |*J. Org. Chem.* 2011, 76, 1821–1830

due to the different priority order of the surrounding groups. In addition, it may be worth pointing out that although four palmarumycins with a chlorine atom, namely palmarumycins C_1, C_4, C_7, and C_8,[5] were reported previously, their structures are quite different from those of compounds **5** and **6**. Biogenetically, the chlorinated derivatives **5** and **6** may be obtained by the nondiastereoselective α chlorination of the ketone derivative **1** followed by diastereoselective reduction of the C-1 carbonyl group. Detailed information about the biosynthesis of spirodioxynaphthalenes has been well summarized in our recent review paper.[1] The discovery of compounds **1**−**8** has added to an extremely diverse and complex array of spirodioxynaphthalenes that are rapidly expanding.

The CD analysis of these compounds revealed that their chiroptical properties are determined by both the central chirality elements and the helicity of the fused nonaromatic ring. It also allowed to establish correlations between their absolute geometries and optical parameters, which may serve as reference for the configurational assignment of related derivative in the future.

The real producer of spirodioxynaphthalenes is a matter worthy of discussion. Although those intriguing compounds are generally considered as fungal metabolites, there have been four reports on the isolation of palamrumycins (or preussomerins) from plants: bipendensin from *Afzelia bipendensis*,[24] palmarumycins JC1 and JC2 from *Jatropha curcas*,[19] palmarumycins JC1−2 (which were proposed to be fungal metabolites), isodiospyrin, and isodiospyrol A from *Diospyros ehretioides*,[20] and palmarumycin JC2 from *Dendrobium crystallinum*.[22] In the present work, because compounds **1**−**8** were obtained in a quite appreciable quantities (total amount: 122 mg from 2.8 kg of the leaves and stems), this fact indicates that these compounds should be produced by *B. gymnorrhiza*, though we could not rule out the possibility that they are endophytic or epiphytes fungus metabolites. Further studies should be conducted to prove the real biosynthetic origin of these compounds, as well as to understand their real ecological roles played in the life cycle of the plant.

EXPERIMENTAL SECTION

Plant Material. A specimen of *B. gymnorrhiza* was collected at the Zhanjiang mangrove national nature reserve, Guangdong Province, People's Republic of China, in August 2008 and identified by Associate Prof. Jin-Gui Shen of the Shanghai Institute of Materia Medica, Chinese Academy of Sciences. A voucher specimen (no. 0808-P-41) is available for inspection at the Herbarium of Shanghai Institute of Materia Medica, CAS.

Extraction and Isolation. The air-dried powder of the leaves and stems of *B. gymnorrhiza* (2.8 kg) were exhaustively extracted with MeOH (3 × 7 L) at rt for 1 week. The MeOH extracts were combined and then concentrated in vacuo to give a residue (160.0 g) that was suspended in H_2O (1.5 L) and then partitioned sequentially with EtOAc (3 × 1.5 L) and *n*-BuOH (3 × 1.5 L) to ultimately afford an EtOAc-soluble fraction (80.0 g) and *n*-BuOH-soluble fraction (25.0 g), respectively. The EtOAc-soluble fraction was subjected to silica gel CC eluted with petroleum ether/EtOAc in linear gradient (90:10, 80:20, 70:30, 50:50, 30:70) followed by $CHCl_3$/MeOH in linear gradient (90:10, 80:20, 70:30, 60:40, 0:100) to obtain 14 fractions (fractions 1−14) on the basis of TLC checking. Fractions 10−12 showed interesting dark blue TLC spots after spraying with H_2SO_4. These fractions were mixed together as fraction 10, which was purified by Sephadex LH-20 (petroleum ether/$CHCl_3$/MeOH, 2:1:1) first to give four subfractions (fractions 10.1−10.4). Fraction 10.3 (200.0 mg) was further purified by CC on silica gel ($CHCl_3$/MeOH, 99:1) to give **1** (25.3 mg) and **8** (4.1 mg). Compounds **2** (4.0 mg), **3** (3.5 mg), **5** (71.0 mg), and **6** (2.0 mg) were obtained from fraction 10.4 on CC silica gel eluted with $CHCl_3$/MeOH (97:3 to 95:5). The *n*-BuOH-soluble fraction was subjected first to Sephadex LH-20 CC ($CHCl_3$/MeOH, 1:1) and then separation by silica gel CC ($CHCl_3$/MeOH, 96:4 to 90:10), resulting in compounds **4** (5.0 mg) and **7** (6.0 mg).

(3*R*)-Palmarumycin BG1 (1):. yellow solid; $[\alpha]^{17}_D$ − 151.0 (c = 0.5, $CHCl_3$); palmarumycin JC2:[19] $[\alpha]^{25}_D$ +131.9 (c = 0.5, $CHCl_3$); UV (MeOH) λ_{max} (log ε) 224 (156.9), 256 (20.8), 299 (22.0), 313 (21.7), 327 (22.5) nm; ECD (MeOH), λ [nm] ($\Delta\varepsilon$) ($c = 1.76 \times 10^{-4}$) 345sh (−1.23), 328 (−2.78), 320sh (−1.34), 298sh (−0.77), 284sh (−1.02), 251 (−5.94), 226 (−54.9), 209 (22.91); IR (KBr) ν_{max} 3432, 3058, 2919, 1641, 1608, 1585, 1456, 1413, 1378, 1269, 1164, 1120, 1070, 1027, 977, 821, 756 cm^{-1}; ^1H and ^{13}C NMR (see Tables 1 and 2); selected HMBC data, H-2 → C-1, 3, 4, 10; H-3 → C-1, 2, 4, 5; H-6 → C-1, 4, 5, 7, 8, 9, 10; OH-9 → C-1, 7, 8, 9, 10; ESIMS m/z 335 $[M + H]^+$, 333 $[M - H]^-$; HRESIMS m/z 357.0737 $[M + Na]^+$ (calcd for $C_{20}H_{14}O_5Na$, 357.0739).

(1*S*,3*R*)-Palmarumycin BG2 (2):. white solid; $[\alpha]^{16}_D$ −40 (c = 0.055, $CHCl_3$); ECD (MeOH), λ [nm] ($\Delta\varepsilon$) ($c = 7.4 \times 10^{-4}$) 331 (0.18), 327 (−0.41), 319sh (−0.33), 312sh (−0.63), 298 (−0.83), 283sh (−0.78), 229 (−19.73), 219sh (−4.27), 209 (4.73), 204 (6.17); ^1H and ^{13}C NMR (see Tables 1 and 2); selected HMBC data, H-1 → C-2, 3, 10; H-2 → C-1, 3, 4, 10; H-3 → C-1, 2, 4, 5; H-6 → C-4, 5, 7, 8, 9, 10; H-7 → C-5, 6, 8, 9, 10; H-8 → C-6, 7, 9, 10; ESIMS m/z 359 $[M + Na]^+$, 695 $[2\,M + Na]^+$, 335 $[M - H]^-$; EIMS m/z (rel int) 336 $[M]^+$ (20), 318 $[M - H_2O]^+$ (60), 302 (20), 271(10), 160 (76), 159 (100),149 (37), 131 (70), 121 (30), 115 (20), 97 (18), 85 (20), 71 (28), 57 (40); HREIMS m/z 336.0998 $[M]^+$ (calcd for $C_{20}H_{16}O_5$, 336.0998).

Palmarumycin BG3 (3):. white solid; $[\alpha]^{17}_D$ −261 (c = 0.14, acetone); ECD (MeOH), λ [nm] ($\Delta\varepsilon$) ($c = 2.62 \times 10^{-4}$) 331 (0.04), 327 (−0.56), 320sh (−0.31), 312sh (−0.52), 298sh (−0.62), 288 (−0.89), 257 (0.12), 247sh (−0.21), 227 (−22.34), 217sh (−5.82), 197 (17.20); IR (KBr) ν_{max} 3592, 3469, 3145, 2921, 2852, 1637, 1606, 1585, 1413, 1378, 1270, 1114, 756; ^1H and ^{13}C NMR (see Tables 1 and 2); selected HMBC data, H-1 → C-2, 3, 9, 10; H-2 → C-1, 3, 4, 10; H-3 → C-1, 2, 4, 5; H-6 → C-4, 5, 7, 8, 9, 10; H-7 → C-5, 6, 8, 9, 10; H-8 → C-6, 7, 9, 10; ESIMS m/z 359 $[M + Na]^+$, 695 $[2\,M + Na]^+$, 335 $[M - H]^-$; HRESIMS 359.0915 $[M + Na]^+$ (calcd for $C_{20}H_{16}O_5Na$, 359.0895).

Palmarumycin BG4 (4):. white solid; $[\alpha]^{16}_D$ +101 (c = 0.1, MeOH); UV (MeOH) λ_{max} (log ε) 226 (37.0), 301 (7.3), 314 (5.6), 328 (4.1); ECD (MeOH), λ [nm] ($\Delta\varepsilon$) ($c = 1.86 \times 10^{-4}$) 330 (0.13), 322sh (0.18), 314sh (0.21), 303 (0.37), 288 (0.27), 276 (−0.29), 267 (−0.26), 257 (0.27), 232 (−6.04), 211 (11.78) nm; IR (KBr) ν_{max} 3400, 2919, 2850, 1645, 1608, 1461, 1413, 1382, 1259, 1033, 970, 896, 819, 754 cm^{-1}; ^1H and ^{13}C NMR (see Tables 1 and 2); selected HMBC data, H-1 → C-2, 3, 9, 10; H-2 → C-1, 3, 4, 10; H-3 → C-1, 2, 4; H-6 → C-4, 5, 7, 8, 9, 10; H-7 → C-5, 6, 8, 9, 10; H-8 → C-6, 7, 9, 10; ESIMS m/z 439 $[M + Na]^+$, 416 $[M]^-$, 415 $[M - H]^-$; HRESIMS 415.0476 $[M - H]^-$ (calcd for $C_{20}H_{15}O_8S$, 415.0488).

Palmarumycin BG5 (5):. brown solid; $[\alpha]^{16}_D$ −314.7 (c = 0.75, $CHCl_3$); UV (MeOH) λ_{max} (log ε) 226 (127.3), 287 (23.1), 299 (21.8), 313 (15.3), 327 (10.2) nm; ECD (MeOH), λ [nm] ($\Delta\varepsilon$) ($c = 1.99 \times 10^{-4}$) 327 (−1.60), 320sh (−0.95), 312 (−1.51), 299 (−1.62), 288sh (−1.41), 250sh (−0.84), 227 (−42.74), 210sh (−11.62), 194 (27.34); IR (KBr) ν_{max} 3384, 2919, 2850, 1637, 1608, 1587, 1463, 1413, 1378, 1270, 1107, 1022, 891, 821, 756, 688 cm^{-1}; ^1H and ^{13}C NMR (see Tables 1 and 2); selected HMBC data, H-1 → C-2, 10; H-2 → C-3, 4; H-3 → C-1, 2, 4, 5; H-6 → C-4, 5, 7, 8, 10; H-7 → C-5, 6, 8, 9; H-8 → C-6, 9, 10; EIMS m/z 372 $[M]^+$ (19), 370 $[M]^+$ (59), 352 $[M - H_2O]^+$ (10), 318 (24), 317 (56), 316 (34), 288 (25), 160 (65), 159 (100), 147 (28), 131 (43), 115 (20), 83 (82); ESIMS m/z 393 $[M + Na]^+$, 763 $[2\,M + Na]^+$, 369 $[M - H]^-$; HRESIMS 393.0521 $[M + Na]^+$ (calcd for $C_{20}H_{15}O_5ClNa$, 393.0506).

Palmarumycin BG6 (6):. brown solid; $[\alpha]^{16}_D$ +60 (c = 0.04, $CHCl_3$); ECD (MeOH), λ [nm] ($\Delta\varepsilon$) ($c = 0.50 \times 10^{-4}$) 329 (1.61), 322sh (0.85), 314 (1.35), 306sh (0.93), 301 (1.17), 295sh (0.76), 279 (− 0.94), 252 (1.18), 246sh (0.67), 232 (− 7.63), 211 (28.15); ^1H and ^{13}C NMR (see Tables 1 and 2); selected HMBC data, H-1 → C-2, 10;

H-2 → C-3, 4; H-3 → C-1, 2, 4, 5; H-6 → C-4, 5, 7, 8, 10; H-7 → C-5, 6, 8, 9; H-8 → C-6, 9, 10; EIMS *m/z* 372 $[M]^+$ (24), 370 $[M]^+$ (76), 352 $[M - H_2O]^+$ (10), 334 $[M - Cl]^+$ (16), 318 (26), 317 (56), 316 (64), 288 (24), 287 (16), 175 (16), 160 (58), 159 (85), 147 (28), 131 (30), 111 (33), 97 (53) 83 (44), 71 (53), 57 (100); ESIMS *m/z* 393 $[M + Na]^+$, 763 $[2M + Na]^+$; HRESIMS 393.0508 $[M + Na]^+$ (calcd for $C_{20}H_{15}O_5ClNa$, 393.0506).

Palmarumycin BG7 (7):. brown solid; $[\alpha]^{17}_D$ − 171 (*c* = 0.1, MeOH); ECD (MeOH), λ [nm] (Δε) (*c* = 3.33 × 10^{-4}) 327 (− 0.48), 320sh (−0.28), 312 (−0.43), 298 (−0.53), 288sh (−0.46), 278sh (−0.43), 226 (−14.50), 211 (−3.39), 193 (8.11); ^1H and ^{13}C NMR (see Tables 1 and 2); selected HMBC data, H-1 → C-2, 5, 9, 10; H-2 → C-3, 4; H-3 → C-1, 2, 4, 5; H-6 → C-4, 5, 7, 8, 10; H-7 → C-5, 6, 8, 9; H-8 → C-6, 9, 10; ESIMS *m/z* 449 $[M - H]^-$ (100), 451 $[M - H]^-$ (35), 415 $[M - Cl]^-$ (17), 371 $[M - SO_3H]^-$ (77); HRESIMS 449.0097 $[M - H]^-$ (calcd for $C_{20}H_{14}O_8SCl$, 449.0098).

Preussomerin BG1 (8):. yellow solid; $[\alpha]^{17}_D$ −135 (*c* = 0.13, $CHCl_3$); UV (MeOH) λ_{max} (log ε) 257 (16.5), 311 (5.2), 357 (5.0) nm; ECD (MeOH), λ [nm] (Δε) (*c* = 2.59 × 10^{-4}) 354sh (−1.22), 332 (−2.01), 270 (−2.19), 251 (1.29), 236sh (−4.45), 217 (−38.47), 193 (38.48); IR (KBr) ν_{max} 3401, 2962, 2923, 2852, 1687, 1650, 1592, 1469, 1261, 1091, 1037, 937, 802 cm^{-1}; ^1H and ^{13}C NMR (see Tables 1 and 2); ESIMS *m/z* 367 $[M + H]^+$, 365 $[M - H]^-$; EIMS *m/z* 366 $[M]^+$ (84), 348 (13), 337 (25), 238 (12), 192 (15), 182 (100), 181 (68), 176 (25), 167 (18), 151 (36), 149 (25), 139 (19), 77 (24), 69 (18), 59(36); HREIMS *m/z* 366.0742 $[M]^+$ (calcd for $C_{20}H_{14}O_7$, 366.0740).

Computational Details. Mixed torsional/low mode conformational searches were carried out by means of the Macromodel 9.7.211[25] software using the Merck molecular force field (MMFF) with implicit solvent model for chloroform. In each conformational search, the maximum number of steps were set to 30000. Geometry reoptimizations at the B3LYP/6-31G(d) level of theory applying no or PCM solvent model for chloroform followed by TDDFT CD calculations using various functionals (B3LYP, BH&HLYP, CAM-B3LYP) and TZVP basis set were performed by the Gaussian 03[26] and the Gaussian 09[27] packages. Boltzman distributions were estimated from the ZPVE-corrected B3LYP/6-31G(d) energies of the optimized conformer geometries obtained at the same level of theory in the gas-phase calculations, and from the B3LYP/6-31G(d) energies in the PCM calculations. CD spectra were generated as the sum of Gaussians[28] with 3000, 2100, and 1200 cm^{-1} half-height width (corresponding to ca. 15, 10, and 6 at 220 nm, respectively), using dipole-velocity computed rotational strengths. The MOLEKEL[29] software package was used for visualization of the results.

■ ASSOCIATED CONTENT

Supporting Information. 1D and 2D NMR and HREIMS spectra of all compounds; DFT-optimized geometry of **3**, **4**, and **6**; experimental CD spectrum of (1*R*,2*S*,3*S*)-**6**. This material is available free of charge via the Internet at http://pubs.acs.org.

■ AUTHOR INFORMATION

Corresponding Author

*(Y.-W.G.) E-mail: ywguo@mail.shcnc.ac.cn. Tel: +86-21-50805813. Fax: +86-21-50805813. (T.K.) E-mail: kurtant@tigris.klte.hu. Tel: (36) 52 316 666/22466. Fax: 36 52 453 836.

■ ACKNOWLEDGMENT

This research work was financially supported by the National S & T Major Project (Nos. 2009ZX09301-001, 2009ZX09103-060), National Marine 863 Program for Druggability Evaluation (2011-2013), the Natural Science Foundation of China (Nos. 30730108, 21021063, 40976048, 81072572), the STCSM Project (09ZR1438000, 10540702900), and the CAS Key Project (SIMM0907KF-09), and was partially funded by a grant from CAS (KSCX2-YW-R-18) and EU 7th framework Programme (IRSES project 2010-2014). The computational stereochemical studies were supported by the National Office for Research and Technology (NKTH, K-68429).

■ REFERENCES

(1) Cai, Y.-S.; Guo, Y.-W.; Krohn, K. *Nat. Prod. Rep.* **2010**, *27*, 1840–1870.
(2) Weber, H. A.; Baenziger, N. C.; Gloer, J. B. *J. Am. Chem. Soc.* **1990**, *112*, 6718–6719.
(3) Weber, H. A.; Gloer, J. B. *J. Org. Chem.* **1991**, *56*, 4355–4360.
(4) (a) Ogishi, H.; Chiba, N.; Mikawa, T.; Sasaki, T.; Miyaji, S.; Sezaki, M.; JP 01, 294, 686, 1989; *Chem. Abstr.*, **1990**, *113*, 38906q. (b) Krohn, K.; Michel, A.; Flörke, U.; Aust, H. J.; Draeger, S.; Schulz, B. *Liebigs Ann. Chem.* **1994**, 1093–1097.
(5) Krohn, K.; Michel, A.; Flörke, U.; Aust, H. J.; Draeger, S.; Schulz, B. *Liebigs Ann. Chem.* **1994**, 1099–1108.
(6) Singh, S. B.; Zink, D. L.; Liesch, J. M.; Ball, R. G.; Goetz, M. A.; Bolessa, E. A.; Giacobbe, R. A.; Silverman, K. C.; Bills, G. F.; Pelaez, F.; Cascales, C.; Gibbs, J. B.; Lingham, R. B. *J. Org. Chem.* **1994**, *59*, 6296–6302.
(7) Schlingmann, G.; West, R. R.; Milne, L.; Pearce, J.; Carter, G. T. *Tetrahedron Lett.* **1993**, *34*, 7225–7228.
(8) Jiao, P.; Swenson, D. C.; Gloer, J. B.; Campbell, J.; Shearer, C. A. *J. Nat. Prod.* **2006**, *69*, 1667–1671.
(9) Hu, H. J.; Guo, H. J.; Li, E. W.; Liu, X. Z.; Zhou, Y. G.; Che, Y. S. *J. Nat. Prod.* **2006**, *69*, 1672–1675.
(10) Dong, J. Y.; Song, H. C.; Li, J. H.; Tang, Y. S.; Sun, R.; Wang, L.; Zhou, Y. P.; Wang, L. M.; Shen, K. Z.; Wang, C. R.; Zhang, K. Q. *J. Nat. Prod.* **2008**, *71*, 952–956.
(11) Martínez-Luis, S.; Della-Togna, G.; Coley, P. D.; Kursar, T. A.; Gerwick, W. H.; Cubilla-Rios, L. *J. Nat. Prod.* **2008**, *71*, 2011–2014.
(12) Pai, J.-K.; Frank, E. A.; Blood, C.; Chu, M. *Anti-Cancer Drug Des.* **1994**, *9*, 363–372.
(13) (a) Chu, M.; Truumees, I.; Patel, M.; Gullo, V. P.; Blood, C.; King, I.; Pai, J.-K.; Puar, M. S. *Tetrahedron Lett.* **1994**, *35*, 1343–1346. (b) Chu, M.; Truumees, I.; Patel, M. G.; Gullo, V. P.; Puar, M. S. *J. Org. Chem.* **1994**, *59*, 1222–1223. (c) der Sar, S. A.; Blunt, J. W.; Munro, M. H. G. *Org. Lett.* **2006**, *8*, 2059–2061. (d) Chen, X. M.; Shi, Q. Y.; Lin, G.; Guo, S. X.; Yang, J. S. *J. Nat. Prod.* **2009**, *72*, 1712–1715.
(14) Sun, Y.-Q.; Guo, Y.-W. *Tetrahedron Lett.* **2004**, *45*, 5533–5535.
(15) Gong, J.-X.; Shen, X.; Yao, L.-G.; Jiang, H.-L.; Krohn, K.; Guo, Y.-W. *Org. Lett.* **2007**, *9*, 1715–1716.
(16) Liu, H.-L.; Shen, X.; Jiang, H.-L; Guo, Y.-W. *Chin. J. Org. Chem.* **2008**, *28*, 246–251.
(17) Gong, J.-X.; Shen, X.; Yao, L.-G.; Jiang, H.-L.; Krohn, K.; Guo, Y.-W. *Chin. J. Org. Chem.* **2008**, *28*, 252–255.
(18) Huang, X.-Y.; Wang, Q.; Liu, H.-L.; Zhang, Y.; Xin, G.-R.; Dong, M.-L.; Guo, Y.-W. *Phytochemistry* **2009**, *70*, 2096–2100.
(19) Ravindranath, N.; Reddy, M. R.; Mahender, G.; Ramu, R.; Kumar, K. R.; Das, B. *Phytochemistry* **2004**, *65*, 2387–2390.
(20) Prajouklang, A.; Sirithunyalug, B.; Charoenchai, P.; Suvannakad, R.; Sriubolmas, N.; Piyamongkol, S.; Kongsaeree, P.; Kittakoop, P. *Chem. Biodiversity* **2005**, *2*, 1358–1367.
(21) Bode, H. B.; Walker, M.; Zeek, A. *Eur. J. Org. Chem.* **2000**, *42*, 3185–3193.
(22) Wang, L.; Zhang, C.-F.; Wang, Z.-T.; Zhang, M.; Xu, L.-S. *J. Asian Nat. Prod. Res.* **2009**, *11*, 903–911.
(23) Krohn, K.; Flörke, U.; John, M.; Root, N.; Steingrover, K.; Aust, H.-J.; Draeger, S.; Schulz, B.; Antus, S.; Simonyi, M.; Zsila, F. *Tetrahedron* **2001**, *57*, 4343–4348.
(24) Kouam, T. N. M.; Lavaud, C.; Massiot, G.; Nuzillard, J. M.; Connolly, J. D.; Ryeroft, D. S. *Nat. Prod. Lett.* **1993**, *3*, 299–303.

(25) (a) Mohamadi, F.; Richard, N. G. J.; Guida, W. C.; Liskamp, R.; Lipton, M.; Caufield, C.; Chang, G.; Hendrickson, T.; Still, W. C. *J. Comput. Chem.* **1990**, *11*, 440–467.(b) MacroModel, Schrödinger LLC, 2009. http://www.schrodinger.com/Products/macromodel.html.

(26) Frisch, M. J.; Trucks, G. W.; Schlegel, H. B.; Scuseria, G. E.; Robb, M. A.; Cheeseman, J. R.; Montgomery, J. A., Jr.; Vreven, T.; Kudin, K. N.; Burant, J. C.; Millam, J. M.; Iyengar, S. S.; Tomasi, J.; Barone, V.; Mennucci, B.; Cossi, M.; Scalmani, G.; Rega, N.; Petersson, G. A.; Nakatsuji, H.; Hada, M.; Ehara, M.; Toyota, K.; Fukuda, R.; Hasegawa, J.; Ishida, M.; Nakajima, T.; Honda, Y.; Kitao, O.; Nakai, H.; Klene, M.; Li, X.; Knox, J. E.; Hratchian, H. P.; Cross, J. B.; Bakken, V.; Adamo, C.; Jaramillo, J.; Gomperts, R.; Stratmann, R. E.; Yazyev, O.; Austin, A. J.; Cammi, R.; Pomelli, C.; Ochterski, J. W.; Ayala, P. Y.; Morokuma, K.; Voth, G. A.; Salvador, P.; Dannenberg, J. J.; Zakrzewski, V. G.; Dapprich, S.; Daniels, A. D.; Strain, M. C.; Farkas, O.; Malick, D. K.; Rabuck, A. D.; Raghavachari, K.; Foresman, J. B.; Ortiz, J. V.; Cui, Q.; Baboul, A. G.; Clifford, S.; Cioslowski, J.; Stefanov, B. B.; Liu, G.; Liashenko, A.; Piskorz, P.; Komaromi, I.; Martin, R. L.; Fox, D. J.; Keith, T.; Al-Laham, M. A.; Peng, C. Y.; Nanayakkara, A.; Challacombe, M.; Gill, P. M. W.; Johnson, B.; Chen, W.; Wong, M. W.; Gonzalez, C.; Pople, J. A. Gaussian 03, Revision C.02., Gaussian, Inc., Wallingford, CT, 2004.

(27) Frisch, M. J.; Trucks, G. W.; Schlegel, H. B.; Scuseria, G. E.; Robb, M. A.; Cheeseman, J. R.; Scalmani, G.; Barone, V; Mennucci, B.; Petersson, G. A.; Nakatsuji, H.; Caricato, M.; Li, X.; Hratchian, H. P.; Izmaylov, A. F.; Bloino, J.; Zheng, G.; Sonnenberg, J. L.; Hada, M.; Ehara, M.; Toyota, K.; Fukuda, R.; Hasegawa, J.; Ishida, M.; Nakajima, T.; Honda, Y.; Kitao, O.; Nakai, H.; Vreven, T.; Montgomery, J. A.; Peralta, J. E., Jr.; Ogliaro, F.; Bearpark, M.; Heyd, J. J.; Brothers, E.; Kudin, K. N.; Staroverov, V. N.; Kobayashi, R.; Normand, J.; Raghavachari, K.; Rendell, A.; Burant, J. C.; Iyengar, S. S.; Tomasi, J.; Cossi, M.; Rega, N.; Millam, J. M.; Klene, M.; Knox, J. E.; Cross, J. B.; Bakken, V.; Adamo, C.; Jaramillo, J.; Gomperts, R.; Stratmann, R. E.; Yazyev, O.; Austin, A. J.; Cammi, R.; Pomelli, C.; Ochterski, J. W.; Martin, R. L.; Morokuma, K.; Zakrzewski, V. G.; Voth, G. A.; Salvador, P.; Dannenberg, J. J.; Dapprich, S.; Daniels, A. D.; Farkas, O.; Foresman, J. B.; Ortiz, J. V.; Cioslowski, J.; Fox, D. J. Gaussian 09, Revision A.02, Gaussian, Inc., Wallingford, CT, 2009.

(28) Stephens, P. J.; Harada, N. *Chirality* **2010**, *22*, 229–233.

(29) Flükiger, P.; Lüthi, H. P.; Portmann, S.; Weber, J.; MOLEKEL 5.4., 2000−2002, Swiss Center for Scientific Computing, Manno, Switzerland.